Aerosol and Air Quality Research, 14: 708–724, 2014
Copyright © Taiwan Association for Aerosol Research
ISSN: 1680-8584 print / 2071-1409 online
doi: 10.4209/aaqr.2013.05.0163

Impact of Biomass Burning on Aerosol Size Distribution, Aerosol Optical Properties and Associated Radiative Forcing

Elisabeth Alonso-Blanco[1], Ana I. Calvo[2], Véronique Pont[3], Marc Mallet[3], Roberto Fraile[4*], Amaya Castro[4]

[1] *Centro de Investigaciones Energéticas, Tecnológicas y Ambientales (CIEMAT), 28040 Madrid, Spain*
[2] *Centre for Environmental and Marine Studies (CESAM), University of Aveiro, 3810-193 Aveiro, Portugal*
[3] *Laboratoire d'Aérologie/OMP, UMR 5560, Université de Toulouse III, CNRS-UPS, 14, av. E. Belin, 31400 Toulouse, France*
[4] *Departamento de Física. IMARENAB. Universidad de León, 24071 León, Spain*

ABSTRACT

The influence of biomass burning on aerosol size distributions, particle number and radiative forcing has been studied at a rural site in Spain. It has been found that air contaminated by aerosols from biomass burning presents four times the total number of particles registered in non-contaminated air. In the case of the smallest fraction of the fine mode, between 0.1 and 0.2 μm, the increase soars to over seven times the total number of particles. An analysis of the evolution of the count mean diameter in the fine mode (CMD_f) in the 8 daily measurements has revealed a decrease of over 25% in this parameter in the modified measurements when compared with measurements that were not contaminated by aerosols from biomass burning. In contrast, when the aerosol transport time is long, the increases detected in CMD_f range between 15% and 100% when compared with measurements of air by non-aged aerosol from biomass burning. Shortwave radiative forcings have been calculated for these high loads of fine aerosols with GAME (Global Atmospheric Model) software. For the August event, the daytime average of surface radiative forcing is –66 (±30) W/m^2, and at the top of the atmosphere the forcing is –32 (±12) W/m^2. Induced daytime average of atmospheric radiative forcing reaches 34 (±20) W/m^2. The study demonstrates that wildfires affect not only the number of particles and the size distribution, causing a clear increase in the number of aerosols in the atmosphere, but they are also responsible for altering the local radiative balance.

Keywords: Aerosol optical counter; Aerosol optical properties; Aerosol size distribution; Biomass burning; Radiative forcing.

INTRODUCTION

Biomass burning, both natural and man-induced, is an aggressive phenomenon which releases large amounts of particles and gases into the atmosphere, altering its composition at local, regional and even global scales. The consequences that may be triggered in the atmosphere by biomass burning depend mainly on the type of fuel and its characteristics, the relative humidity and the wind conditions (Reid *et al.*, 2005).

Together with fossil fuel burning, biomass burning is the main source releasing carbon aerosols into the atmosphere (IPCC, 2001). During combustion, the elements released cause an increase in the concentrations of particles belonging to the fine mode (particles less than 1 μm) (Cachier *et al.*, 1995; Remer *et al.*, 1998; Reid and Hobbs, 1998; Dubovik *et al.*, 2002), since between 80 and 90% of the particles released by biomass burning correspond to this mode (Reid *et al.*, 2005). These are mainly organic particles, containing mostly organic carbon (OC) and black carbon (BC) (IPCC, 2001), with inorganic traces of sulfates, nitrates, inorganic nutrients and metals, which all together amount to approximately 10% of the particle mass (Cachier *et al.*, 1995).

The different aerosol-mixing states lead to important variations in the hygroscopicity of particles from biomass burning (Cocker *et al.*, 2001; Vakeva *et al.*, 2002; Aklilu *et al.*, 2006; Engelhart *et al.*, 2012). Engelhart *et al.* (2012) have observed a clear positive correlation between the hygroscopicity of these particles and the inorganic mass fraction of the aerosol. The values of the hygroscopicity parameter, k found range between 0.006 (slightly hygroscopic) and 0.6 (highly hygroscopic), where k represents a quantitative measure of aerosol water uptake characteristics. It is defined through its effects on the water activity of the solution.

Many studies have focused on the hygroscopicity of aerosols from burning processes and their efficiency as

* Corresponding author.
Tel.: +34 987 291543; Fax: +34 987 291943
E-mail address: roberto.fraile@unileon.es

Cloud Condensation Nuclei (CCN) (Warner and Twomey, 1967; Eagan *et al.*, 1974; Roberts *et al.*, 2002; Martins *et al.*, 2009). Warner and Twomey (1967), Eagan *et al.* (1974) and Roberts *et al.* (2002) have concluded that, in the case of supersaturations of over 0.5%, particles from wildfires may act as condensation nuclei. Petters *et al.* (2009) have found that aerosols from burning processes are CCN active irrespective of the changes they may undergo later in the atmosphere. Engelhart *et al.* (2012) have found a convergence of the efficiency of aerosols from biomass burning in the formation of CCN after photochemical ageing processes.

Indirect and semi-direct radiative forcings estimates are part of the main current concerns and it is expected that the uncertainties on estimated radiative and climatic impacts should be reduced and our understanding of it improved (IPPC, 2007). Direct radiative forcings have been also widely documented depending on aerosol sources (Hodzic *et al.*, 2007; Mallet *et al*, 2008, 2009; Malavelle *et al.*, 2011). The inferred significant decrease of solar energy at the surface may strongly modify the surface energy budget. Latent heat and sensible heat fluxes from the surface are consequently disturbed as shown by Feingold *et al.* (2005) or Pere *et al.* (2011). The reduction in surface latent and sensible heat fluxes associated with biomass burning impact could reduce cloudiness (Jiang and Feingold, 2006).

In addition to the climate changes that may be caused by aerosols generated by biomass burning, we must also consider the negative impact of aerosols onto human health as they result in poorer air quality. The entrance and deposition of these particles in the respiratory tract depends on the size/surface proportion of the particles and on the ageing conditions involved (Oberdärster *et al.*, 2005). The smaller particles are the ones that enter the respiratory system more easily, reaching even the alveolar region (EPA, 2002). The conditions of the respiratory tract, with a relative humidity close to saturation, trigger a number of changes in the particles inhaled. Londahl *et al.* (2008) have studied the increase in size of aerosols from biomass burning as a result of the high levels of humidity in the respiratory system. It was found that the hygroscopic increase suffered by the particles from combustion processes coincides with the minimum size required for the deposition of these particles in the respiratory tract.

The current study shows the changes in aerosol size distribution registered in a rural area during four summer days with intense biomass burning events. The study events have been registered in the province of León, Spain, and the distance between the wildfires and the sampling point ranged between only a few km and a maximum of 90 km.

Once we identified the cases in which the smoke plumes from the various wildfires (a clearly defined and located source of aerosols) reach the sampling point, the study of the aerosol size distributions revealed the origin and the type of air mass that keeps the particulate matter in suspension before it reaches the sampling point (Calvo *et al.*, 2010a). Afterwards, we estimated the optical properties of the aerosols using the Mie theory. Thus, the Single Scattering Albedo (SSA) and the asymmetry parameter (g) were estimated by the GAME (Global Atmospheric Model) radiative transfer model to compute the instantaneous clear-sky direct radiative forcing (Calvo *et al.*, 2010b).

STUDY ZONE

The province of León is the largest in the region of Castilla y León, Spain, with a total land area of 15,581 km^2. The climate is Mediterranean, with Continental influences, and with a few traces of Atlantic influence too, thus leading to a wide range of different landscapes. In the summer, the province of León is one of the areas most widely affected by wildfires, considering both the number of fires and the total land area burned.

Most of these fires are human-induced. The statistics provided by the regional government Junta de Castilla y León state that 90% of all the wildfires registered are caused by man, be it intentionally or as a result of carelessness.

The measurements analyzed in this paper have been carried out in the district of Carrizo de la Ribera (42°35′6″N 5°49′53″O), 26 km to the north-west of the city of León, Spain (42°35′59″N 5°34′18″O). This is a rural area on the right bank of the River Órbigo, at an altitude of 873 m.

The weather station installed by the Spanish National Agency for Meteorology (AEMET, in its Spanish acronym) in this area (42°35′N, 5°39′W) reflects a Mediterranean but continentalized climate, with a clearly marked seasonality. More detailed information about this study zone has been reported by Alonso-Blanco *et al.* (2011).

MATERIALS AND METHODS

Measurement Equipment

To determine the aerosol size spectrum in this rural area a probe was installed in a field about two km from the town (42°35′59.90″N, 5°50′50.92″W). This laser spectrometer, a Passive Cavity Aerosol Spectrometer Probe, PMS Model PCASP-X, measures particle optical diameter nominally ranging between 0.1 and 10 μm, by considering the light dispersion properties of the particles at a wavelength of 633 nm collected between the angles 35° and 135°. The probe classifies the particle diameter into 31 channels, i.e., 31 intervals of discreet particle sizes. The device was calibrated by the manufacturer using polystyrene latex (PSL) particles of a known size. The refractive index of latex beads (1.59–0i) is different from that of atmospheric particles, resulting in an aerosol size distribution that is "PSL size equivalent".

In this study, we are presenting PCASP-X size distributions adjusted using Mie theory and implemented with a computer code developed by Bohren and Huffman (1983). In the case of the measurements of air that was not contaminated by aerosols from biomass burning, the correction was carried out according to the refractive index typical for rural aerosol, whose values vary depending on the relative humidity (Kim and Boatman, 1990). And in the case of the measurements of air that was contaminated by aerosols from biomass burning, the object of this study, the adjustment was carried out considering a specific refractive index for aerosols from biomass burning.

The study period comprises 4 days, the 13th and 14th of

August and the 3rd and 4th of September 2001. The particle size spectrum was measured 8 times daily, during 10-minute intervals, every 3 hours. The specific refractive index for aerosols from biomass burning was computed by interpolating the real and the imaginary part according to the relative humidity at the time of the measurement (values between 34% and 100%). For the measurements of air containing aerosols from biomass burning the refractive index used has been 1.49–0.013*i*, obtained by Calvo *et al.* (2010b) from the AERONET sunphotometer retrieval at 675 nm for the wildfire detected in Palencia (41°N, 4°W) on the 8th of August 2003.

The refractive indices for aerosols from biomass burning reported in the literature take a range of different values. This is due to the fact that the refractive index depends on the size of the aerosol, the mixing state, the wavelength (λ) at which the index is estimated and the water content of the particles (Seinfeld and Pandis, 1998). In the case of aerosols from biomass burning, one of the most important factors to consider when it comes to estimate the refractive index is the relationship between EC/OC, which determines in turn the relationship between absorption/dispersion of the radiation by the aerosol (IPCC, 2001). Guyon *et al.* (2003) have found an average refractive index -at a value of λ of 545 nm- of 1.41–0.013*i* for particles from biomass burning in the Amazon rainforest. Dubovik *et al.* (2002) have estimated for biomass burning smoke in the Amazon forest –for the visible spectrum of wavelengths– a refractive index with a real part with values between 1.47 and 1.52 and an imaginary part with values between 0.00093 and 0.021. The refractive index found for aerosols in Palencia (1.49–0.013*i*), the one used in this study, is located within this range of values found by Dubovik *et al.* (2002).

In our case study, the choice of the refractive index was determined by the proximity of the study zone to Palencia, an area with a similar topography and vegetation, both natural and of anthropic origin, and with similar characteristics in the wildfires occurring in both areas.

It was also necessary to carry out several corrections on the number of counts sampled by the spectrometer in each channel. Firstly, the flow measurement value was set in relation to the altitude of the sampling point. In the present study the probe was installed at an altitude of 873 m and a correction factor of 0.905 was introduced. In addition, each measurement had to be adjusted with a correction factor to account for coincidence losses at high concentrations. These corrections are described in detail in Calvo *et al.* (2010b).

A weather station was installed next to the probe to register automatically data on precipitation, pressure, temperature, relative humidity and wind speed and wind direction. A wind profiler Sodar SR 1000 was also installed in the same field, with a pulse frequency of 5 tones, about 2150 Hz, a pulse power of 300 W, 8 s pulse-repetition time and a maximum range of 1250 m. This device provided an automatic recording of the wind vector in its three components. The data recorded by the weather station and the Sodar were stored every 30 minutes.

Thermal Inversions, Backward Trajectories and Circulation Weather Type Classification

Three additional aspects have been analyzed to implement the study: the thermal inversions, the backward trajectories of the air masses, and the circulation weather type classification. The thermal inversions were computed from the data obtained by the radiosoundings carried out in La Coruña (43.36°N, 8.41°W, altitude 67 m), Madrid (40.50°N, 3.58°W, altitude 633 m) and Santander (43.48°N, 3.80°W, altitude 59 m) at 1200 and 0000 UTC, and provided by the University of Wyoming (http://weather.uwyo.edu/upperair/sounding.html).

In order to identify the weather type associated with a particular synoptic situation, a circulation weather type classification (CWTs) was set up based on Jenkinson and Collison (1977) and Jones *et al.* (1993). These procedures were developed to define objectively Lamb weather types (Lamb, 1972) for the British Isles. The daily circulation affecting the Iberian Peninsula is described using a set of indices associated to the direction and vorticity of the geostrophic flow. The indices used were the following: southerly flow, westerly flow, total flow, southerly shear vorticity, westerly shear vorticity and total shear vorticity. These indices were computed using sea level pressure values obtained for 16 grid points distributed across the Iberian Peninsula. This method allows for a maximum of 26 different CWTs. Following Trigo and DaCamara (2000) in their study for Portugal, this study does not have a separate class for unclassified days, but has opted for disseminating the fairly few cases with possible unclassified situations (< 2%) among the retained classes. This classification has been used previously for the Iberian Peninsula with a number of different applications, such as the study of lightning (Tomas *et al.*, 2004), splash erosion (Fernandez-Raga *et al.*, 2010), aerosol size distribution in precipitation events (Castro *et al.*, 2010; Calvo *et al.*, 2012) or in studies on precipitation (Fernandez-Gonzalez *et al.*, 2012).

To establish the provenance of the air masses reaching the study zone, back trajectories of 120 h (5 days) have been used, computed at 500 m, 1500 m and 3000 m AGL with the HYSPLIT model -HYbrid Single-Particle Lagrangian Integrated Trajectory Model- by NOAA (Draxler and Rolph, 2003). The HYSPLIT model (Draxler and Hess, 1998) carries out a wide range of simulations related to the long-range transport, dispersion and deposition of air pollutants. The model has been developed by the NOAA Air Resources Laboratory in Maryland, USA. This study will be complemented by a description of these air masses.

Radiative Forcing: Global Atmospheric Model (GAME)

Aerosol-related optical parameters such as Atmospheric Optical Depth (AOD), Single Scattering Albedo (SSA) and the asymmetry parameter (g) are necessary to perform radiative transfer calculations. The last two parameters listed above are not measured directly, so we estimate them via the Mie theory by taking into account the measured aerosol size distribution and the estimated refractive index, representative of a mean chemical composition for biomass burning aerosol. In that way, optical properties are estimated as though the aerosol population was internally mixed. SSA and g are estimated at the seven wavelengths used in the

GAME radiative transfer model. As for the AOD parameter, we have used MODIS data for August 13th and 14th 2001 and for September 3rd and 4th 2001 over the study region at a wavelength of 550 nm.

Once the necessary parameters have been gathered, the spectral optical properties are modeled. Table 1 gives the single scattering albedo and the asymmetry parameter for specific wavelengths (400 nm, 550 nm and 950 nm) and for total size distribution.

The instantaneous clear-sky direct radiative forcing has been estimated with the GAME radiative transfer model detailed in Dubuisson *et al.* (2004). GAME accounts for the scattering and absorption processes by particles and gases. Gaseous absorption (H_2O, CO_2, O_2 and O_3) is treated from the correlated k-distribution, using a line by line code (Dubuisson *et al.*, 1996), and multiple scattering effects are treated using the Discrete Ordinates Method (DOM) (Stamnes *et al.*, 1988). This method allows for accurate treatment of scattering and absorption by aerosols, clouds and molecules. Upward and downward net radiative fluxes are calculated over the spectral solar range, from 2,500 to 50,000 cm^{-1}, with a 100 cm^{-1} spectral resolution. Calculations of radiative fluxes integrated over the entire shortwave region are performed at the specific sampling time.

From these fluxes, we have computed the aerosol clear-sky daily direct forcing at the bottom of the atmosphere (BOA), ΔFBOA, and at the top of the atmosphere (TOA, 20 km in this case), ΔFTOA, defined as mentioned below. The first one represents the effect of particles on the net shortwave radiation fluxes reaching the surface and the second one the radiation fluxes reflected back to space by aerosols. ΔBOA and ΔTOA forcings have been calculated as follows:

$$\Delta FBOA = FBOA(w)^{\downarrow} - FBOA(o)^{\downarrow} \quad (1)$$

$$\Delta FTOA = -(FTOA(w)^{\uparrow} - FTOA(o)^{\uparrow}) \quad (2)$$

where $FBOA(w)^{\downarrow}$ and $FBOA(o)^{\downarrow}$ are, respectively, the downward net radiative fluxes simulated at the surface with (w) and without (o) aerosols. $FTOA(w)^{\uparrow}$ and $FTOA(o)^{\uparrow}$ are, respectively, the upwards net radiative fluxes simulated at the top of atmosphere with (w) and without (o) aerosols. With this convention, a positive sign of ΔF implies a warming effect. Finally, we compute the atmospheric forcing, ΔFATM, by using the following relation:

$$\Delta FATM = \Delta FTOA - \Delta FBOA \quad (3)$$

where ΔFATM represents the possible absorption of solar radiation due to the absorbing properties of fire particles within the atmospheric layer where aerosols are located.

Methodology

The Department for the Environment of the regional government Junta de Castilla y León provided a database with information on the number of fires per day, the district where each fire occurred, the date of detection and extinction (with the exact day and time), and the total land area affected in hectares (ha) with the type of vegetation burned. This information was used to draw maps of the province of

Table 1. Single Scattering Albedo (SSA) and asymmetry parameter (*g*) on August 13th and 14th 2001 and September 3rd and 4th 2001 at 0700, 1000, 1300, 1600 and 1900 UTC for 400 nm, 550 nm and 950 nm wavelengths.

AOD	Data (Day/Time)		Optical Properties					
			SSA			*g*		
			Wavelengths (nm)			Wavelengths (nm)		
			400	550	950	400	550	950
0.6	13/08/2001	0700 UTC	0.961	0.950	0.917	0.594	0.512	0.434
	13/08/2001	1000 UTC	0.957	0.945	0.923	0.587	0.509	0.497
	13/08/2001	1300 UTC	0.948	0.923	0.861	0.494	0.396	0.404
	13/08/2001	1600 UTC	0.942	0.922	0.900	0.545	0.487	0.539
	13/08/2001	1900 UTC	0.951	0.936	0.927	0.614	0.538	0.568
0.4	14/08/2001	0700 UTC	0.964	0.955	0.929	0.613	0.531	0.451
	14/08/2001	1000 UTC	0.944	0.932	0.929	0.629	0.576	0.599
	14/08/2001	1300 UTC	0.953	0.938	0.920	0.595	0.515	0.529
	14/08/2001	1600 UTC	0.953	0.938	0.920	0.595	0.515	0.529
	14/08/2001	1900 UTC	0.941	0.926	0.918	0.631	0.577	0.602
0.4	3/09/2001	0700 UTC	0.981	0.977	0.976	0.675	0.620	0.648
	3/09/2001	1000 UTC	0.956	0.946	0.931	0.622	0.553	0.535
	3/09/2001	1300 UTC	0.956	0.944	0.927	0.589	0.515	0.524
	3/09/2001	1600 UTC	0.951	0.934	0.908	0.550	0.465	0.502
	3/09/2001	1900 UTC	0.948	0.930	0.913	0.561	0.491	0.548
0.4	4/09/2001	0700 UTC	1.000	1.000	1.000	0.760	0.710	0.620
	4/09/2001	1000 UTC	0.968	0.962	0.942	0.656	0.594	0.483
	4/09/2001	1300 UTC	0.963	0.954	0.928	0.622	0.548	0.458
	4/09/2001	1600 UTC	0.958	0.947	0.917	0.607	0.527	0.461
	4/09/2001	1900 UTC	0.964	0.956	0.928	0.631	0.556	0.443

León with all the districts affected by wildfires on the study days and the days immediately before, i.e., on the 12th, 13th and 14th of August and on the 2nd, 3rd and 4th of September 2001.

The maps and the data on the wind direction at surface level and a certain altitude registered by the weather station and the Sodar enabled us to determine which measurements carried out by the PCASP were affected by the transport of smoke plumes from the surrounding wildfires.

The particle records of the 8 daily measurements were compared with the life time of the wildfires, from the time of detection until the time of extinction. Considering the evolution in the number of particles, it was possible to establish the time at which the smoke plume arrived at the sampling point because the corresponding measurements presented very large numbers of particles, reaching a fourfold increase when compared with the other measurements carried out the same day but not affected by the smoke. Once the measurements that might have been affected by the smoke plumes had been identified, the first data selection was obtained by checking the wind speed and direction at that time and the distance between the wildfire and the probe. Subsequently, the second data selection was made with the non-parametric test of Mann-Whitney for a significance level of 0.05 (Essenwanger, 1986), with the purpose of identifying those measures of air affected by aerosols from wildfires. For that reason, the measures previous to those affected by aerosols from wildfires have been used as background.

The weather conditions on the study days have been characterized by analyzing the atmospheric stability considering the circulation weather type, thermal inversions and the corresponding air masses.

The aerosol size distribution on the study days has been analyzed in detail by checking the evolution of the count mean diameter in the fine mode and the number of particles corresponding to this size range in the 8 daily measurements. The clear-sky instantaneous direct radiative forcing of the aerosols released has been studied too, both at the bottom of the atmosphere (ΔFBOA) and at the top of the atmosphere (ΔFTOA), as well as the atmospheric forcing (ΔFATM).

RESULTS AND DISCUSSION

Meteorological Analysis

The meteorological characteristics of the 4 study days, 13th and 14th of August and 3rd and 4th of September 2001, are shown in Table 2. The average monthly temperatures are typical of the summer months. The highest values are found on the 13th and 14th of August with 22.1°C and 18.9°C, respectively. Lower values were recorded on the 3rd and 4th of September, with 16.5°C and 15.9°C, respectively. The maximum and minimum temperatures follow a similar trend: around 30°C and 15°C, respectively, for the days in August, and around 25°C and 7°C, respectively, for the days in September. In general, the temperature parameters show a decreasing trend along the summer, typical for this season in these latitudes.

The daily precipitation registered in the study period is very low: only 0.2 mm in the two study days in August.

Table 2. Meteorological study of the 13th and 14th of August and 3rd and 4th of September 2001, with data on maximum, minimum and average temperatures, relative humidity, wind intensity and total precipitation registered and circulation weather type (CWT) classification and radiative and subsidence thermal inversions. (-) means data not available.

Day	T_{max} (°C)	T_{min} (°C)	T_{av} (°C)	HR (%)	Wind (m/s)	P_{total} (mm)	CWT	Thermal Inversions					
								Madrid 00 UTC		La Coruña 00 UTC		Santander 00 UTC	
								Radiative (m AGL)	Subsidence (m AGL)	Radiative (m AGL)	Subsidence (m AGL)	Radiative (m AGL)	Subsidence (m AGL)
13th August	30.7	15.1	22.1	60.6	1.5	0.2	N			-	-		
14th August	28.7	13.4	18.9	65.0	1.6	0.2	NW		441		473	238	594
3rd September	26.8	8.5	16.5	71.1	1.7	0	NE	55				51	
4th September	25.5	6.7	15.9	76.3	0.7	0	NE		471		970	42	734

The average relative humidity ranges between 60 and 77%, with the highest values registered on the 3rd and 4th of September. The average wind speed was moderate, with less than 2 m/s on average every day. On the 4th of September the wind speed registered remained under 1 m/s.

Circulation Weather Types, Thermal Inversions and Air Masses

The CWT classification shows that during the study days of August and September (Table 2), the CWTs were three: the purely northern type (N) on the 13th of August, the purely north-western type (NW) on the 14th of August, and the purely north-eastern type (NE) on the 3rd and 4th of September. The air masses that reach the Iberian Peninsula on the study days came from the north. However, on the 13th and 14th of August these air masses had a clearly maritime influence, and on the 3rd and 4th of September they had a clearly continental influence.

On the 14th of August no thermal inversions were registered in the soundings carried out in Madrid and Santander at 0000 UTC and there are no data on this issue in the sounding carried out in La Coruña at 0000 UTC. In contrast, in the other 3 study days thermal inversions are common, both radiative and subsidence inversions at altitudes under 1000 meters AGL. There are even moments when both types coexist, thus generating an isolating layer that delays the dispersion of the smoke plumes from the various wildfires. Consequently, there is a high concentration of aerosols in the layer closest to the surface. As for the soundings carried out at 1200 UTC in La Coruña, Madrid and Santander, no data for the study days are available.

The back trajectories (Fig. 1) have drawn for the study days at three altitudes (500, 1500 and 3000 m AGL) reveal different situations. On the 13th of August the high pressure systems around the Iberian Peninsula generate a saddle point in the study zone. On that day, the back trajectories show a clear atmospheric instability (Fig. 1(a)) and the aerosols registered at two altitudes, 500 and 1500 m, come from the surface (in the 6 hours immediately before the meaurement). This indicates that the aerosols from the wildfires joined the air mass that reached the probe. On the 14th of August the situation tends to stabilize; the air masses bring to the study zone marine and continental aerosols, and at 500 m there are also surface level aerosols in the 6 hours immediately before the arrival of the air mass to the sampling site (Fig. 1(b)). On the 3rd and 4th of September (Figs. 1(c) and 1(d)) the air mass reaching the Iberian Peninsula is a maritime polar (mP) air mass. This air mass brings with it maritime aerosols and is characterized for being cold and wet, thus explaining the decrease in temperature and the increase in the relative humidity registered on these days when compared to the study days in the month of August.

Characterization of the Wildfires

This section describes the wildfires registered during the study days (13th and 14th of August and 3rd and 4th of September), as well as the ones registered on the previous days, the 12th of August and the 2nd of September, respectively. These wildfires altered the local atmospheric composition and some of them contaminated the aerosols measurements carried out on the 13th and 14th of August and on the 3rd and 4th of September.

On the 12th of August, 10 wildfires were registered and a total land area of 244 ha was burned. Of these fires, 5 were very small (the burned surface is S < 1 ha), and 5 were medium-sized (500 ha > S > 1 ha). Three of the medium-sized fires originated to the north-west of the study zone, within a radius of 90 km, and burned 239 ha, 98% of the land area affected that day. All the fires detected on the 12th of August were extinguished that same day.

On the 13th and 14th of August, 19 and 18 wildfires were registered, respectively. A total of 37 fires burned 517 ha. Of these, 26 were very small and 11 of a medium size. Of the medium-sized fires, 2 started within a radius of 75 km to the south-west of the study zone and burned 93% of the surface affected those days, a total of 479 ha. Both fires were detected on the 13th of August and were extinguished on the 14th.

On the 2nd of September, the day immediately before our two study days (3rd and 4th of September), 7 wildfires burned a total area of 143 ha. Of these, only one was of small size and the other 6 were medium-sized. Two of the medium-sized fires started within a radius of 95 km to the north-west of the study zone and burned 134 ha, 94% of the surface burned that day. Both fires started and were extinguished on the 2nd of September, coexisting in time.

On the 3rd and 4th of September there were a total of 11 wildfires: 9 on the 3rd of September and 2 on the 4th of September, burning together 65 ha. Of the total number of wildfires, 5 were small and the rest medium-sized. Two of the medium-sized fires burned 65 ha, 80% of the surface burned those days. Both fires were detected on the 3rd of September, within a radius of 75 km, to the south-west of the study zone. The medium-sized fire affecting a smaller area, 17 ha, was extinguised on that same day, but the other one affected a much larger area, 35 ha, and could not be extinguished until the 4th of September.

In general, the wildfires detected during the study days ranged during daytime, between 1200 UTC and 2200 UTC. Few fires are detected outside this time range. The wildfires registered on these days are mainly located to the west and south-west of the study area. The zones affected are mostly in the mountains, at altitudes of around 1000 m, surrounded by valuable landscapes.

The smoke plumes of the medium-sized wildfires affecting considerable amounts of land may be carried long distances by the wind (Fraile *et al.*, 2006), at least to a regional scale. In our study they are responsible for the important increases in the number of aerosols registered in the sampling point, installed in a rural area.

Influence of Biomass Burning on Aerosol Measurements

Aerosol Size Distributions

The multi-log-normal function was used to characterize the size distributions of aerosol particles (e.g., Whitby, 1978; Hoppel *et al.*, 1994). It thus becomes very easy to compare several data sets of aerosol particles. The multi-log-normal concept is thoroughly described in the literature

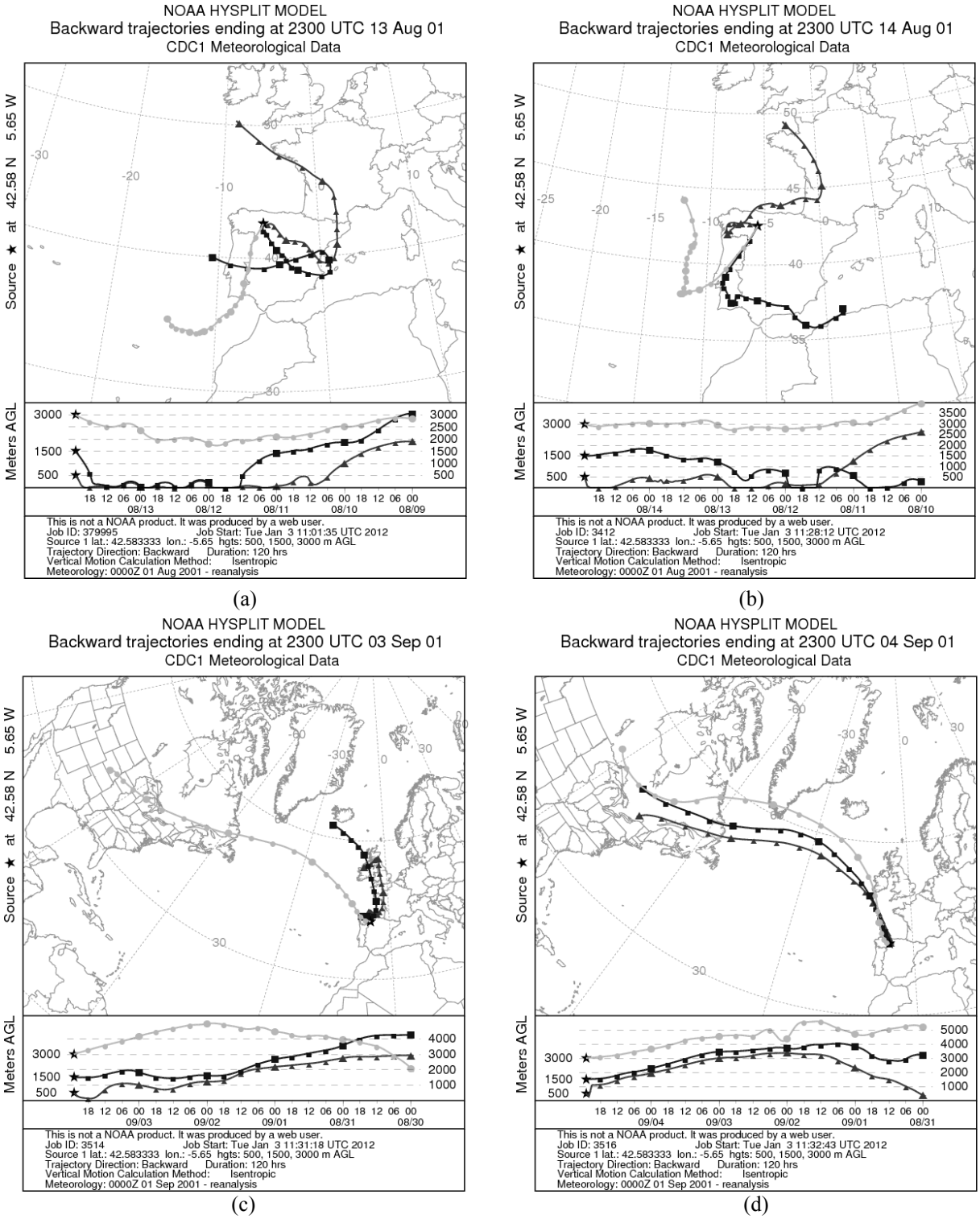

Fig. 1. Back trajectories for three different altitudes (500, 1500 and 3000 m) using the HYSPLIT model on (a) 13th, (b) 14th of August and (c) 3rd and (d) 4th of September 2001.

and the overall outcome has proven to be useful whenever parameterizations are required (e.g., Mäkelä *et al.*, 2000; Birmili *et al.*, 2001).

It was found that the size distributions analyzed by the PCASP-X were bimodal: with a fine and a coarse mode. Fig. 2 shows the aerosol size distributions on the study days. During the wildfires registered on the study days, we observed a clear increase in the number of particles smaller than 0.2 μm in the measurements contaminated by the smoke plumes. Increases of up to seven times were recorded in this size range. The same situation was found by Janhall *et al.* (2010) in fresh smoke from biomass burning,

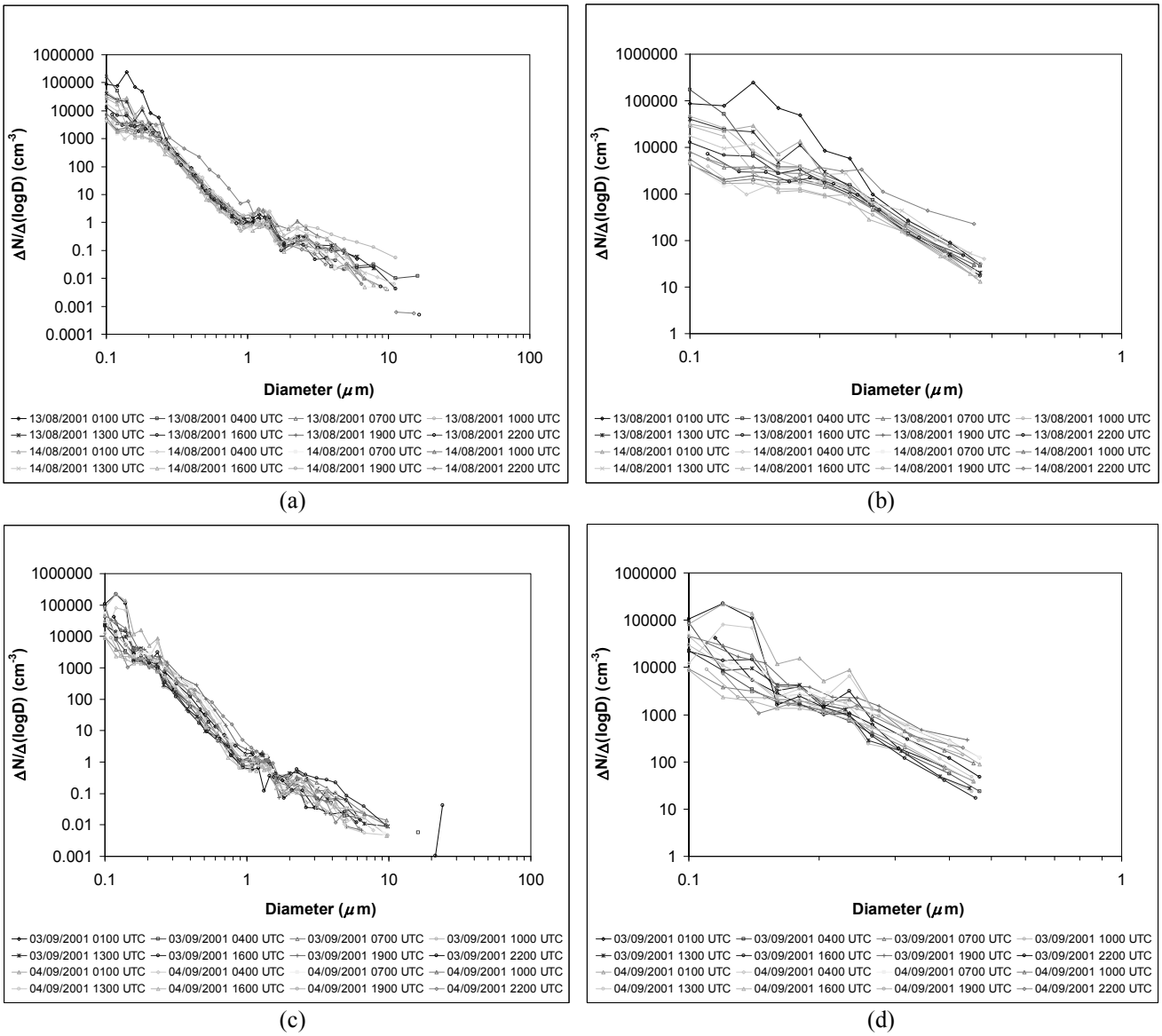

Fig. 2. Aerosol size distributions of air contaminated by aerosols from biomass burning registered in the 8 daily measurements on the (a and b) 13th and 14th of August and (c and d) 3rd and 4th of September 2001, for the fine and the coarse mode, and for sizes under < 0.5 μm.

recording an increase in the number of particles in the fine mode by an arithmetic mean with a standard deviation of the Geometric Mean Diameter of 117 ± 13 nm. Kleeman *et al.* (1999), in a study on particle mass distributions of fresh smoke from wood burning, estimate a mode centered in a range of particle size between 0.1–0.2 μm.

The application of non parametric test of Mann-Whitney measures allowed us to identify those ones affected by aerosols from wildfires. Since the increases observed in the number of particles correspond to minor sizes of 0.2 μm, the test has been executed for the first five channels corresponding to this size. Thanks to these results, it has identified five measures of air contaminated on the 13th of August, one measure on the 14th of August and one and three measures on the 3rd and 4th September, respectively.

During the event comprising the 13th and 14th of August, the measurements affected by wildfires are the ones recorded during the night on the 13th of August (0100 UTC and 0400 UTC) and on the 14th of August (0100 UTC) and the central hours of the 13th of August (1000 UTC, 1300 UTC and 1600 UTC). Particles concentration average increases of 300% were registered in air contaminated by aerosols from biomass burning when compared to previous uncontaminated measurements. At 0100 UTC on both days the measurements exceeded a 400% increase in the particles concentration (Fig. 2(a)). These increases are even more important in the case of particles in the size range between 0.1 and 0.2 μm, exceeding 700% in the particles concentration in some of the measurements.

Of particular importance are the two processes of contamination by aerosols from biomass burning registered on the 13th of August. The first of these events occurred in

the early hours, at 0100 UTC and 0400 UTC, and the figures registered were 35,492 and 19,882 particles/cm^3, respectively. Three hours later, at 0700 UTC, the figures registered were 1734 particles/cm^3. This decrease reflects clearly the evolution of the smoke plume from biomass burning, from its arrival to its dispersion and the subsequent return to normal levels of atmospheric particulate matter.

A similar situation is observed in the second contamination process on the 13th of August, between 0700 UTC and 1600 UTC. At 0700 UTC the number of particles registered is 1734 particles/cm^3. The arrival of a smoke plume to the probe causes a considerable increase in the number of particles at 1000 UTC: 7728 particles/cm^3. The number of particles remains constant at 1300 UTC, with 7712 particles/cm^3, but at 1600 UTC there is a significant decrease in the number of particles: 2546 particles/cm^3. The number of particles of sizes between 0.10–0.12 μm starts increasing at 1000 UTC, with 4873 particles/cm^3, more than four times the number registered in that size range at 0700 UTC. At 1300 UTC this increase in the number of particles spreads to the ones between 0.1 and 0.2 μm, with 2308 particles/cm^3, 40% more than the ones registered at 1000 UTC in the same size range. The return to normal begins at 1600 UTC, with 2444 particles/cm^3, a drop of 67% in the number of particles smaller than 0.2 μm (Fig. 2(b)) when compared to the measurement carried out at 1300 UTC.

On the 13th of August, the measurements were affected by the wildfire in Villagatón, in the district of Astorga. This fire started on the 12nd of August at 1346 UTC and lasted until 2159 UTC the same day. During this period the wind direction was mainly N with an average speed of 1 m/s. The smoke plume took approximately 8 hours to reach the sampling point after the beginning of the fire. In contrast, the measurements affected by aerosols from biomass burning registered on the 14th of August corresponded to a wildfire which started in Santa Colomba de Somoza, also in the district of Astorga, on the 13th of September at 1930 UTC. This fire was extinguished on the 14th of August at 2000 UTC. The average wind speed registered during the fire at the measurement site is 1.7 m/s, with three dominating directions: S, N and NNE. The smoke plume took around 6 hours to reach the probe after the fire started (Table 3).

Figs. 2(c) and 2(d) represent the situation on the 3rd and 4th of September. On the 3rd of September, two measurements were contaminated by aerosols from biomass burning, the one at 0400 UTC, with 9005 particles/cm^3, and the one at 2200 UTC, with 32,961 particles/cm^3. The increases in the number of particles were of 60% and 500%, respectively, when compared to the previous uncontaminated air measurements. The measurement carried out at 2200 UTC includes aerosols from a wildfire in Castrillo de la Cabrera, in the district of Truchas (Table 3), which began on the 3rd of September at 1145 UTC and was extinguished at 1800 UTC that same day, burning a total of 17 ha. During the active life of the wildfire, at surface level the average wind speed is of 3 m/s, mainly of the directions NNE and WNW, so the smoke plume reached the probe in around 6 hours from the beginning of the fire. At 0400 UTC the measurement was affected by aerosols from biomass burning, but it was not

Table 3. Characterization of the wildfires contaminating the measurements carried out on the 13th and 14th of August and on the 3rd and 4th of September 2001, with reference to the sampling point: district where the fire was registered, distance to the sampling point, date of detection and extinction, wind speed and wind direction, estimated time the smoke plume takes to reach the sampling point and total land area burned according to the type of vegetation (Woodland tree, Non-tree Woodland and non-forest Mass), as well as the total land area affected by wildfires altering the local atmospheric composition on the study days.

Day	District	Distance to the sampling point (km)	First Detected		Date of Extinction		Wind (m/s)	Surface wind direction	Time the smoke plume takes to reach the probe (h)	Burned Area (ha)			
			Day	Time (UTC)	Day	Time (UTC)				Woodland tree	Non-tree woodland	Non-forest mass	Total
12th August	Villagatón (42°38′05″N 6°09′43″O)	28	12nd August	1346	12nd August	2159	1	N	8	1	179	0	180
13th and14th August	Santa Colomba de Somoza (42°26′40″N 6°14′39″O)	38	13th August	1930	14th August	2000	1.7	N, NNE, S	6	0	72	0	72
3rd September	Castrillo de Cabrera (42°20′25″N 6°32′39″O)	64	3rd September	1145	3th September	1800	3	NNE, WNW	6	11	6	0	17

possible to determine which fires contaminated that record. It may be the case that aerosols from other fires were registered here too, including fires from the 2nd of September around the study zone, within a radius of 38 to 92 km, since the number of particles measured on that day, excluding the other two contaminated measurements, is of 4147 ± 1394 particles/cm^3, the highest value in the four study days.

On the 4th of September, the wildfire in Castrillo de la Cabrera, in the district of Truchas, is the reason for the high number of particles measured in the early hours of that day, with increases of over 500% when compared with previous measurements, at 0100 and 0400 UTC, registering 34,171 and 12,090 particles/cm^3, respectively. At 0700 UTC, the measurement immediately after the one at 0400 UTC, there were only 7017 particles/cm^3. In other words, as on the 13th of August, the evolution of the number of particles at these times (0100 and 0400 UTC) indicates the arrival of a smoke plume from biomass burning and the later return to the normal levels of particulate matter.

The considerable increases in these days in certain measurements cannot be explained by the presence of a high atmospheric stability, nor by the simultaneous occurrence of radiative and/or subsidence thermal inversions. The only reason is the arrival of smoke plumes from the wildfires registered on those days.

In general, the measurements affected by the wildfires during the study period were the ones carried out during the night (between 2200 UTC and 0400 UTC) and in the central hours of the day (between 1000 UTC and 1600 UTC). The results indicate that the wildfires release to the atmosphere particles of the submicrometric aerosol fraction (fine mode), as shown by Rissler *et al.* (2006). A direct relationship was found between the occurrence of certain wildfires and the increase in the number of particles in some of the measurements. We claim that in the four study days the important wildfire activity is influencing the concentration of the number of particles at a local level, altering more or less the 8 measurements carried out during those days.

The graphs corresponding to the surface and volume size distributions (Fig. 3) and the calculation of Volume Median Diameter (VMD) and Surface Median Diameter (SMD) have been made. In general, it has been observed that the distribution area and volume of air measures affected by aerosols from fires were increased for particles < 0.2 μm and the SMD and VMD are shifted to smaller sizes, indicating that the particles emitted by wildfires correspond to small sizes.

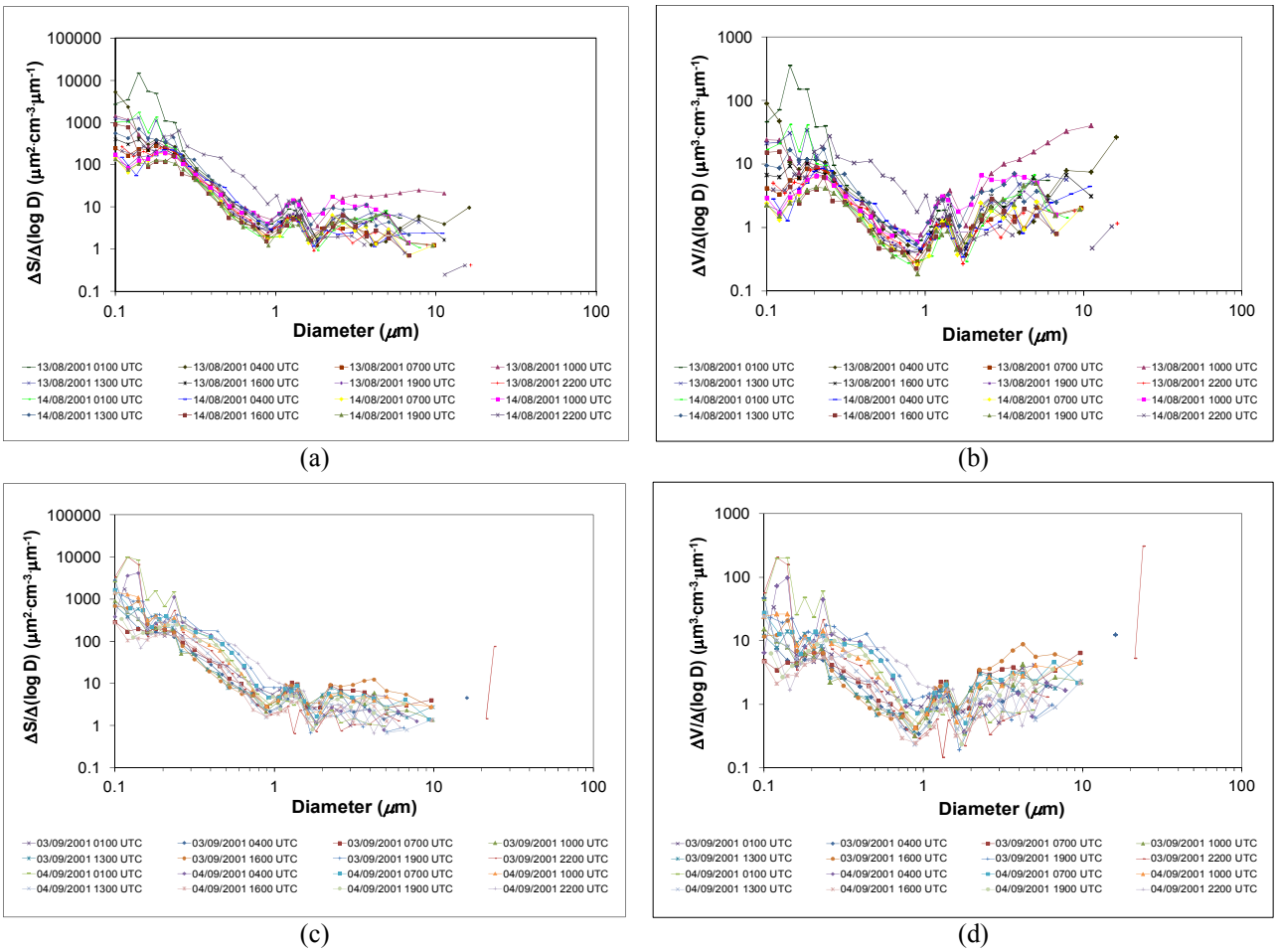

(a) (b) (c) (d)

Fig. 3. Surface and Volume Aerosol size distributions registered in the 8 daily measurements on the (a and b) 13th and 14th of August and (c and d) 3rd and 4th of September 2001.

Daily Evolution: Count Mean Diameter (CMD_f) and Number of Particles in the Fine Mode (N_f)

The role of biomass burning in the characteristics of the particulate matter on the four study days was studied by comparing the evolution along the 8 daily records of the count mean diameter (CMD), and the number of particles. As mentioned above, biomass burning processes cause changes in size distributions, mainly in the smaller fraction of the fine mode. The estimations carried out to determine the daily number of particles in the coarse mode (1–10 µm) indicated that there were very few particles in this size range, around 3 particles/cm^3; therefore, the results focus exclusively on data corresponding to the fine mode (in this study, with PCASP-X only particles between 0.1–1 µm), considering the evolution of the CMD_f and the total number of particles (N_f) (Figs. 4 and 5).

On the 13th of August, the concentration of the number of particles was higher during the night than during the day. The particles registered during the evening also had a larger CMD_f, reaching its maximum at 1900 UTC with a size of 0.15 µm. In daytime the minimum is reached at 1600 UTC with 0.07 µm. All the records presented a high geometric deviation, i.e., particles of very different sizes coexist on the same day.

As for the number of particles in the fine mode, the first measurement contaminated by aerosols from biomass burning was registered at 0100 UTC. In this record the estimation is N_f = 94,025 particles/cm^3. At this time, the CMD_f drops from a value of 0.12 µm at 2200 UTC on the 12th of August to a value of 0.09 µm at 0100 UTC on the 13th of August. In the following measurement at 0400 UTC the CMD_f was 0.10 µm, with a decrease in N_f of 98% (Figs. 4(a) and 4(b)). Between 0700 UTC and 1900 UTC the second contamination process occurred with the arrival of particles from biomass burning. The estimations for N_f were 2716, 3271, 13,629, 7507 and 828 particles/cm^3 for the measurements taken at 0700 UTC, 1000 UTC, 1300 UTC, 1600 UTC and 1900 UTC, respectively. At 0700 UTC and at 1000 UTC the CMD_f was 0.10 µm, later dropping to 0.08 and 0.07 µm at 1300 UTC and 1600 UTC, respectively. By 1900 UTC there was a clear return to normal values, with 0.15 µm.

The data clearly illustrate the fact that the measurements were affected by two smoke plumes from biomass burning, and that they later returned to normal background levels in the content of particulate matter after the smoke plumes dispersed. In addition, the measurements contaminated by aerosol from biomass burning presented a decrease in the CMD_f of more than 25%. Other studies on the CMD of aerosols from biomass burning found slightly higher values. Le Canut *et al.* (1996) found a CMD of 0.125 ± 0.02 µm in emissions of fresh smoke from wildfires in the savannahs in northern Africa. Janhall *et al.* (2010) found a CMD of around 0.120 µm in fresh smoke for three fuel types: forest, savanna and grass. The size of the aerosols during the combustion processes depends mainly on the type of fuel, the availability of oxygen, the temperature of the combustion, and on the phase in the combustion process (flaming phase or smoldering phase) (Reid *et al.*, 2005). The uncertainty generated by instrumental techniques must also be taken into account.

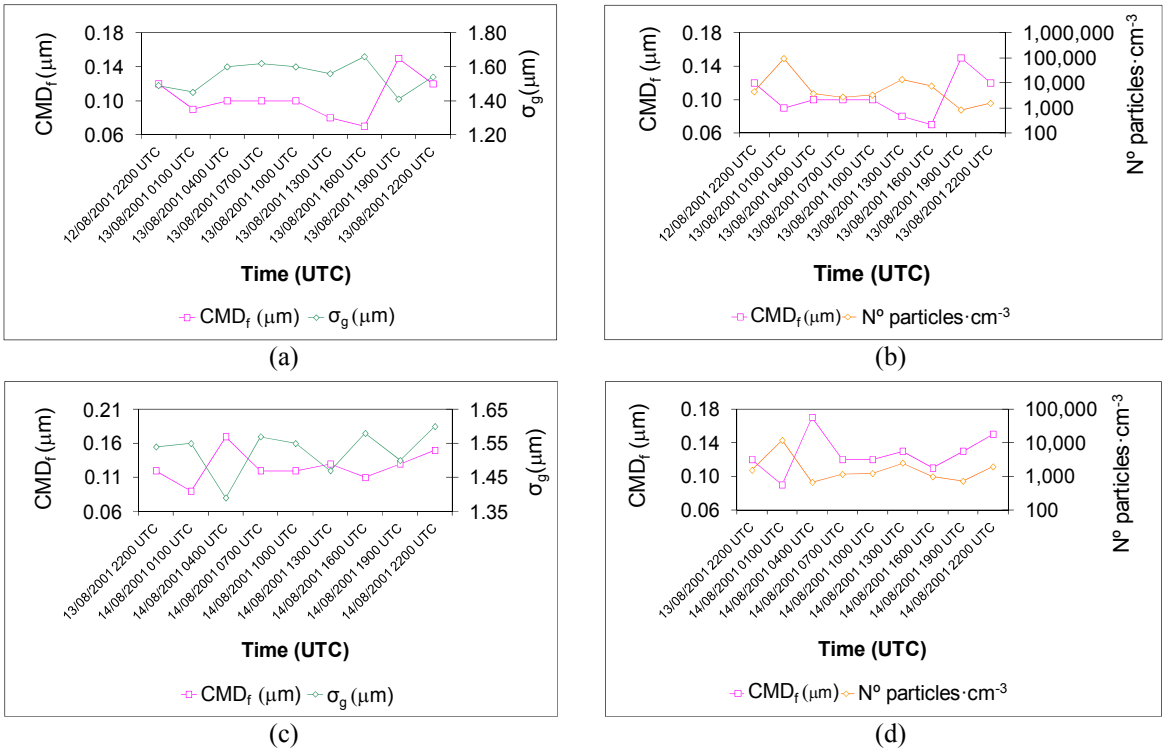

Fig. 4. Comparative analysis of the evolution of the count mean diameter (CMD_f) (left-hand column) and the total number of particles in the fine mode (right-hand column) in the 8 daily measurements on the (a and b) 13th and (c and d) 14th of August 2001.

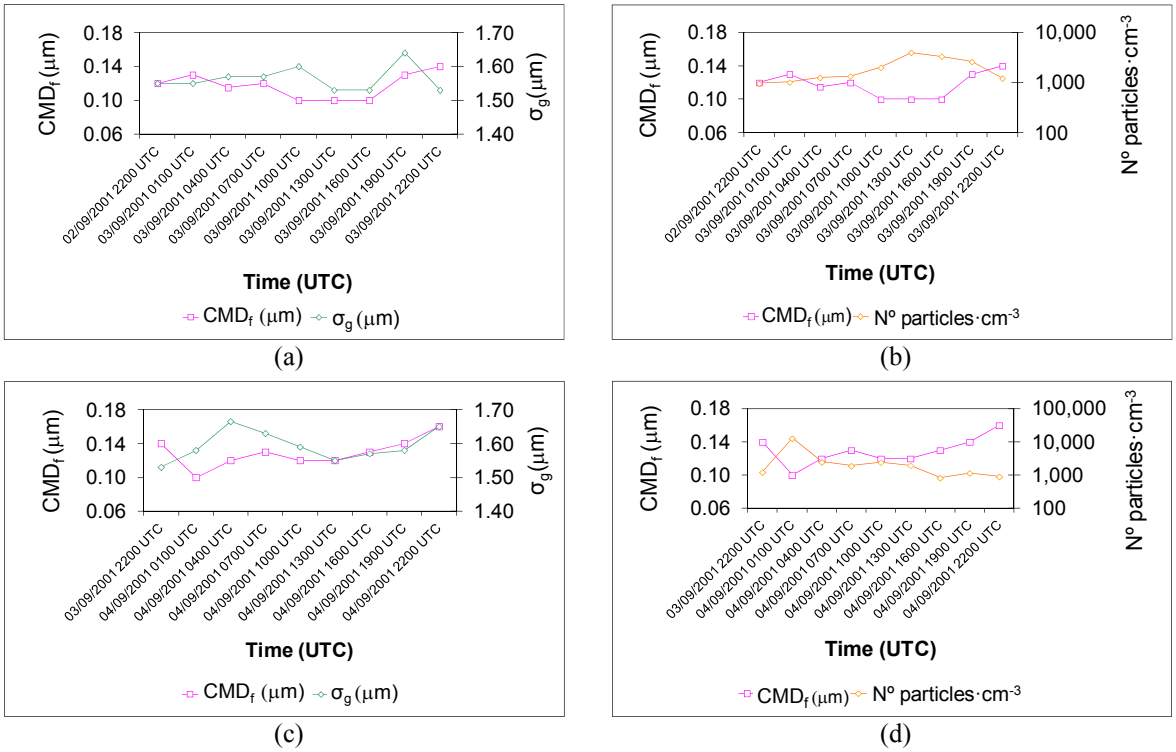

Fig. 5. Comparative analysis of the evolution of the count mean diameter (CMD_f) (left-hand column) and the total number of particles in the fine mode (N_f) (right-hand column) in the 8 daily measurements on the 3rd of September 2001 (a and b) and on the 4th of September 2001 (c and d).

On the 14th of August, during the night, the most important oscillations both in the number of particles and in their sizes were found. The concentration of particles in the fine mode remained more stable during the daytime (0700 UTC to 1900 UTC) (Figs. 4(c) and 4(d)). The minimum CMD_f was reached at 0100 UTC, estimating a value of 0.09 μm, coinciding with the main increase in N_f that day: 11,749 particles/cm^3. The high concentration of particles in the fine mode, together with the low values of the CMD_f, which dropped from 0.12 μm at 2200 UTC on the 13th of August 2001 to 0.09 μm at 0100 UTC on the 14th of August (a 25% decrease) points towards a clear air contamination by the presence of aerosols from biomass burning.

The maximum CMD_f was registered at 0400 UTC with 0.17 μm. During the whole day there was a marked heterogeneity in the size of the particulate matter, with large and small particles coexisting. But at 0400 UTC the low geometric deviation (σ_g) with respect to the previous measurements (1.39 μm) pointed towards more uniform sizes, with the larger fraction of the fine mode dominating. The reason for this situation may have been a greater atmospheric stability during the night leading to the ageing of the aerosols from biomass burning registered at 0100 UTC.

On the 3rd of September the CMD_f was higher during the night than in daytime, with the maximum CMD_f recorded at 2200 UTC, with a value of 0.14 μm. The minimum CMD_f was found between 1000 UTC and 1600 UTC, with a value of 0.10 μm. It was in this time interval that the lowest geometric deviations of the fine mode were registered (1.53 μm). In other words, the particles found in the atmosphere in these hours corresponded to the smallest fraction of the fine mode and had more homogeneous particle sizes. With respect to the number of particles in the fine mode, there were two clearly distinct time intervals: one during the night (from 2200 UTC to 0700 UTC), with a concentration of particulate matter around 1161 ± 163 particles/cm^3, and another one during the day (from 1000 UTC to 1900 UTC), with a higher number of particles estimated at 2971 ± 679 particles/cm^3 (Figs. 5(a) and 5(b)).

The estimated N_f for the measurements contaminated by aerosol from biomass burning (0400 UTC and 2200 UTC) were 1254 and 1221 particles/cm^3, with a CMD_f of 0.12 and 0.14 μm, between 15% and 100% higher than the CMD_f values in the other contaminated measurements in the study period. As mentioned before, on the 3rd of September there was a high concentration of particulate matter during the whole day. The only direct influence observed in the measurement taken at 2200 UTC was the wildfire in Castrillo de la Cabrera, which started on the 3rd of September. The low number of particles in the fine mode, together with the high values of the CMD_f, seems to indicate that the aerosols measured suffered a longer transport from wildfires that occurred on previous days. The atmospheric stability during the night favored aerosol ageing. Some studies focus on characterizing aerosol growth by ageing, associated with long-range transport of the smoke plume. Radke *et al.* (1995) found that during the transport of the smoke plume from the wildfires, the geometric median diameter (GMD) of the aerosols in the fine mode increases

to more than 0.25 μm after 25 h of transport. A more recent study by Eck *et al.* (2003) found that, when the smoke plume remains isolated during the transport and this transport lasts for several days, aerosol ageing processes occur and the values of the peak volume modal radius (*r*) registered lie around 0.20 μm.

On the 4th of September the CMD_f oscillated during the day, with an increasing trend towards the evening. The minimum CMD_f was registered at 1000 UTC with 0.10 μm, and the maximum CMD_f at 2200 UTC with 0.16 μm. The geometric deviation of the fine mode indicated that during the day the particulate matter had more uniform sizes (Fig. 5(c)).

As in the case of the other two study days, the 13th and 14th of August, there was an increase in the number of particles in the fine mode at 0100 UTC, with 12,749 particles/cm^3. This increase coincided with a decrease in the CMD_f in this measurement. The values changed from 0.14 μm at 2200 UTC on the 3rd of September to 0.10 μm at 0100 UTC on the 4th of September. This value tended to increase, and we found a CMD_f of 0.12 μm at 0400 UTC and 0.13 μm at 0700 UTC, with an estimated N_f of 2488 particles/cm^3 and 1907 particles/cm^3, respectively (Fig. 4(d)). At 0100 UTC and 0400 UTC there was a decrease of around 20% in the CMD_f when compared with the measurement taken at 2200 UTC on the 3rd of September, which was not contaminated by aerosols from biomass burning. The CMD_f values obtained that day for aerosols from biomass burning were similar to the ones found by Reid *et al.* (2005) in their study on fresh smoke from various types of biomass burning. This study found that the CMD of the aerosols ranged between 0.1 and 0.13 μm. As mentioned above, the evolution of the CMD_f and the N_f on this day revealed the arrival of a smoke plume from biomass burning and the subsequent return to normal levels afterwards. During the rest of the day the number of particles remained stable with a mean value of 1490 ± 620 particles/cm^3.

The four study days presented very similar trends, with a clear boundary between nighttime (from 1900 UTC, when dusk set in, until 0700 UTC, when the next day dawned) and daytime (from 0700 UTC to 1900 UTC). In the four study days the nocturnal CMD_f presented an increasing trend, whereas during the day it tended to decrease. The same situation was found in a previous study by Alonso-Blanco *et al.* (2011), and it may be linked to a higher atmospheric stability, thus favoring aerosol ageing processes as the particles remain in the atmosphere for longer periods of time.

This situation changed only when the measurements are contaminated by aerosols from biomass burning. At that point, the number of particles estimated for the fine mode (N_f) soared to the highest values registered those days. This situation coincided with average decreases in the CMD_f of over 25% when compared with previous uncontaminated measurements. After the dispersion of the smoke plume, the CMD_f returned to the usual values registered before the arrival of aerosols from biomass burning. In other words, the smoke plumes from the wildfires were releasing into the atmosphere particles belonging to the smallest fraction of the fine mode. With prolonged aerosol transport times, as on the 3rd of September, we found increases in the CMD_f between 15% and 100% when compared with uncontaminated measurements and with shorter transport times (13th and 14th of August and 4th of September).

Aerosols from Biomass Burning in Air Quality Control Regulations

The concentration of PM_{10} particulate matter was estimated taking 1.35 g/cm^3 as the density of particles from biomass burning (Reid and Hobbs, 1998), and assuming that ambient air particles in rural areas have a density of 1 g/cm^3, as found in previous studies by Thatcher and Layton (1994) and Riley *et al.* (2002), who analyzed particulate matter indoors and outdoors in urban and rural areas. In measurements that are not contaminated by aerosols from wildfires the estimated concentrations were under 20 μg/m^3 and in contaminated measurements the estimated concentrations may be of up to 90 μg/m^3, higher than the daily maximum threshold value (24 hours) of 50 μg/m^3 established by European and Spanish Regulations on Air Quality Control (Real Decreto 102/2011 de 28 de enero). This concentration should not be exceeded more than 35 times per year. Barnaba *et al.* (2011), in an exhaustive study carried out in Europe on the contribution of wildfires to atmospheric particulate matter, establish a preliminary estimation of the average monthly contribution of aerosols from biomass burning during the months with more wildfires at levels of 10 μg/m^3. This indicates that wildfires may influence legal controls on air quality.

Influence of Aerosols from Biomass Burning on Aerosol Optical Properties and Associated Radiative Forcing

First, considering the optical properties of aerosols (Table 1) we note the spectral dependence of SSA with high values for short wavelengths. It follows then that the aerosol is mainly light scatterer rather than absorber. Nevertheless, SSA values vary all day long, so the absorption property of the aerosol also varies. Indeed, positive atmospheric radiative forcings (Table 4) result in atmospheric heating by absorbing particles.

Our simulations enabled us to investigate the surface forcing during the fire events. The instantaneous surface forcing estimated by GAME reached up to –98 W/m^2 and –82 W/m^2 during the August and September fire events, respectively (Table 4). The daytime average was –66(±29) W/m^2 for a mean AOD of 0.5 and a refractive index of about 1.48–0.005*i* during the August event, and it was –57 (±23) W/m^2 for a mean AOD of 0.4 and a refractive index of about 1.45–0.004*i* during the September event. Such values are consistent with those simulated by Formenti *et al.* (2002), from the STAAARTE MED 1998 experiment. Indeed, for an AOD of about 0.3, for a refractive index of 1.55–0.025*i*, over sea surface and over sea plus vegetation surface, daytime averages of direct radiative forcing at the surface are, respectively, –55 (±20) W/m^2 and –49 (±16) W/m^2. These average values were of the same order. The lower aerosol loadings in the column 'atmosphere' of the STAAARTE MED experiment (represented by the lower

Table 4. Instantaneous direct radiative forcings (W/m^2) on (a) August 13th and 14th 2001, and (b) September 3rd and 4th 2001, and daytime average of direct radiative forcings.

(a)

DATE (Day/Time)	ΔBOA	ΔTOA	ΔATM
13/08/2001 0700 UTC	–19.2	–16.1	3.1
13/08/2001 1000 UTC	–96.2	–43.2	53.1
13/08/2001 1300 UTC	–93.1	–37.2	55.9
13/08/2001 1600 UTC	–98.3	–50.8	47.5
13/08/2001 1900 UTC	–55.5	–33.2	22.3
14/08/2001 0700 UTC	–17.1	–13.9	3.2
14/08/2001 1000 UTC	–71.1	–26.3	44.8
14/08/2001 1300 UTC	–74.7	–27.2	47.6
14/08/2001 1600 UTC	–77.5	–38.1	39.4
14/08/2001 1900 UTC	–55.5	–33.2	22.3
Daytime Average	–65.8	–31.9	33.9

(b)

DATE (Day/Time)	ΔBOA	ΔTOA	ΔATM
3/09/2001 0700 UTC	–15.6	–14.5	1.1
3/09/2001 1000 UTC	–73.4	–30.3	43.1
3/09/2001 1300 UTC	–73.7	–28.5	45.2
3/09/2001 1600 UTC	–81.8	–41.7	40.1
3/09/2001 1900 UTC	–57.0	–36.6	20.4
4/09/2001 0700 UTC	–16.6	–11.9	4.7
4/09/2001 1000 UTC	–61.2	–31.5	29.6
4/09/2001 1300 UTC	–61.7	–30.6	31.1
4/09/2001 1600 UTC	–71.1	–38.3	32.8
4/09/2001 1900 UTC	–53.8	–36.7	17.1
Daytime Average	–56.6	–30.1	26.5

AOD) seems to be compensated by a more absorbing aerosol as the imaginary part of the refractive index is higher than ours.

Instantaneous ΔFTOA (Table 4) were computed by GAME, reaching up to –51 W/m^2 and –42 W/m^2 during the August and September fire events, respectively. The daytime average of direct radiative forcing at TOA was about –32 (±12) W/m^2 and –30 (±10) W/m^2, respectively. For comparison, these instantaneous values were found to be higher than those obtained by Formenti *et al.* (2002), in the case studies described above, with daytime averages of direct radiative forcing at TOA, respectively, of –21 (±7) W/m^2 and –12 (±5) W/m^2. This difference might be due to the fact that in our case SSA values stand for scattering aerosols. For most of our case studies the aerosol forcing was negative (cooling effect) and much higher at the surface than at the TOA due to absorption.

Besides, positive instantaneous ΔFATM given by GAME illustrate the absorption of solar radiation in the atmosphere by the smoke aerosol considered (Table 4). It reached up to +60 W/m^2 and +45 W/m^2 during the August and September fire events, respectively. These instantaneous values were consistent with those found by Sicard *et al.* (2012) for biomass burning in Barcelona (+60 W/m^2). Our daily average values (Table 4) were consistent with those reported by Hodzic *et al.* (2007), who found that this forcing could reach daily average values of +40 W/m^2 in the fire source region.

Concerning the daily variations of these radiative fluxes, we observed that the direct atmospheric radiative forcing reached maximum values when the fire events occurred at a time of day when the solar radiation available is high. For example, the aerosol number concentration is 6 times higher at 1300 UTC than during the morning for the fine mode on the 13th of August 2001. These high loads of aerosols in the fine mode interacted with shortwave radiation through absorption and scattering processes, which was translated by a lower downward radiative flux reaching the surface (ΔFBOA highly negative). The daily trends of radiative fluxes of our case studies were consistent with those found by Lyamani *et al.* (2006), with both radiative forcings at TOA and BOA increasing (absolute values) with a solar zenith angle of up to about 60° and decreasing absolute values with a solar zenith angle greater than 60°.

CONCLUSIONS

In rural areas wildfires may be considered the main sources of high loads of particles in the atmosphere and clearly alter particle size distributions. The present study has registered increases in the total number of particles of over 4 times when compared with uncontaminated measurements. This increase corresponded mostly to particles in the fine mode, mainly to sizes between 0.1 and 0.2 μm, where the values recorded were up to seven times the values in measurements not contaminated by aerosols from biomass burning. In other words, wildfires release into the atmosphere particles belonging to the smallest fraction of the fine mode.

Excluding the measurements of air contaminated by aerosols from biomass burning, in the 4 study days the count mean diameter of the fine mode (CMD_f) showed a clearly decreasing trend in the registers taken during daytime. In contrast, during the night there was an increase in the CMD_f. It could be due to the processes of ageing or hygroscopicity and deliquescence provoked by the increase of the relative humidity during the night. This difference between daytime and nighttime measurements may be motivated by actual atmospheric dynamics or thermodynamics. During the day the convective processes are more intense, whereas during the night an increased atmospheric stability results in less ventilation, favoring aerosol ageing processes. This situation is only altered with the arrival of aerosols from wildfires, resulting in an increase in the number of particles in the fine mode and a decrease in the CMD_f of more than 25% when compared with the measurement taken immediately before the arrival of the smoke plume. It was also observed that when the aerosols from biomass burning remained in the atmosphere for longer periods of time, the ageing processes and the aerosol hygroscopicity and deliquescence, resulted in increases of the CMD_f between 15% and 100% when compared to contaminated measurements where no ageing processes were detected.

Wildfires are causing atmospheric pollution in rural areas, with PM_{10} concentrations of up to 90 μg/m^3, exceeding by far the daily threshold value of 50 μg/m^3 established by the European and Spanish Regulations for Air Quality Control.

Calculations of surface, top of the atmosphere and

atmospheric radiative forcings with the GAME radiative transfer model reveal a strong attenuation of the shortwave incoming solar radiation at the surface during fire events. Due to high loads of fire aerosols in the atmospheric column related to high AOD and increases in fine mode aerosol concentrations, the instantaneous atmospheric radiative forcings reach high positive values (between 26 and 34 W/m^2) translating an important absorption. These different forcings of direct radiative effects may affect the heating rate in the atmosphere and induce major thermodynamic and microphysical feedbacks. Latent and sensible heat fluxes at surface as well as microphysics in clouds could be modified.

ACKNOWLEDGMENTS

The authors wish to thank Miguel Angel Olguín, from the Department for the Environment of the regional government Junta de Castilla y León, for his assistance whenever it was required. Many thanks go to Dr. Laura López Campano for her co-operation and to Dr. Noelia Ramón for translating the paper into English. The authors are grateful to Darrel Baumgardner for his help with the code developed by Bohern and Huffman. This study was supported by the Spanish Ministry of Science and Innovation (TEC2010-19241-C02-01). Ana I. Calvo acknowledges the posdoc grant SFRH/BPD/64810/2009 from FCT. E. Alonso-Blanco acknowledges the FPI grant to carry out the doctoral thesis/ PhD at the Research Centre for Energy, Environment and Technology (CIEMAT).

REFERENCES

Aklilu, Y., Mozurkewich, M., Prenni, A.J., Kreidenweis, S.M., Alfarra, M.R., Allan, J.D., Anlauf, K., Brook, J., Leaitch, W.R., Sharma, S., Boudries, H. and Worsnop, D.R. (2006). Hygroscopicity of Particles at two Rural, Urban Influenced Sites during Pacific 2001: Comparison with Estimates of Water Uptake from Particle Composition. *Atmos. Environ*. 40: 2650–2661.

Alonso-Blanco, E. Calvo, A.I., Fraile, R. and Castro, A (2012). The Influence of Wildfires on Aerosol Size Distributions in Rural Areas. *Sci. World J.* 2012: ID 735697, doi: 10.1100/2012/735697.

Barnaba, F., Angelini, F., Curci, G. and Gobbi, G.P. (2011). An Important Fingerprint of Wildfires on the European Aerosol Load. *Atmos. Chem. Phys*. 11: 10487–10501.

Birmili, W., Wiedensohler, A., Heintzenberg, J. and Lehmann, K. (2001). Atmospheric Particle Number Size Distribution in Central Europe: Statistical Relations to Air Masses and Meteorology. *J. Geophys. Res*. 106: 32005–32018.

Bohren, C.F. and Huffman, D.R. (1983). *Absorption and Scattering of Light by Small Particles*, Wiley, New York.

Cachier, H., Liousse, C., Buatmenard, P. and Gaudichet, A. (1995). Particulate Content of Savanna Fire Emissions. *J. Atmos. Chem*. 22: 123–148.

Calvo, A.I., Olmo, F.J., Lyamani, H., Alados-Arboledas, L., Castro, A., Fernandez-Raga, M. and Fraile, R. (2010a). Chemical Composition of Wet Precipitation at the Background EMEP Station in Víznar (Granada, Spain) (2002–2006). *Atmos. Res*. 96: 408–420.

Calvo, A.I., Pont, V., Castro, A., Mallet, M., Palencia, C., Roger, J.C., Dubuisson, P. and Fraile, R. (2010b). Radiative forcing of haze during a forest fire in Spain. *J. Geophys. Res.* 115: D08206, doi: 10.1029/2009JD012172.

Calvo, A.I., Pont, V., Olmo, F.J., Castro, A., Alados-Arboledas, L., Vicente, A.M., Fernández-Raga, M. and Fraile, R. (2012). Air Masses and Weather Types: A Useful Tool for Characterizing Precipitation Chemistry and Wet Deposition. *Aerosol Air Qual. Res.* 12: 856–878.

Castro, A., Alonso-Blanco, E., Gonzalez-Colino, M., Calvo, A.I., Fernandez-Raga M. and Fraile R. (2010). Aerosol Size Distribution in Precipitation Events in León. Spain. *Atmos. Res*. 96: 421–435.

Cocker, D.R., Whitlock, N.E. and Flagan, R.C. (2001). Hygroscopic Properties of Pasadena, California Aerosol. *Aerosol Sci. Technol*. 35: 637–647.

Draxler, R.R. and Hess, G.D. (1998). An Overview of the HYSPLIT_4 Modelling System for Trajectories, Dispersion and Deposition. *Aust. Meteorol. Mag*. 47: 295–308.

Draxler, R.R. and Rolph, G.D. (2003). HYSPLIT (HYbrid Single-Particle Lagrangian Integrated Trajectory). Model Access via NOAA ARL READY Website (http://www.arl.noaa.gov/ready/hysplit4.html Last Access: 11 May 2103), NOAA Air Resources Laboratory, Silver Spring, MD.

Dubovik, O., Holben, B., Eck, T.F., Smirnov, A., Kaufman, Y.J., King, M.D., Tanre, D. ans Slutsker, I. (2002). Variability of Absorption and Optical Properties of Key Aerosol Types Observed in Worldwide Locations. *J. Atmos. Sci*. 59: 590–608.

Dubuisson, P., Buriez, J.C. and Fouquart, Y. (1996). High Spectral Resolution Solar Radiative Transfer in Absorbing and Scattering Media: Application to the Satellite Simulation. *J. Quant. Spectrosc. Radiat. Transfer* 55: 103–126.

Dubuisson, P., Dessailly, D., Vesperini, M. and Frouin, R. (2004). Water Vapor Retrieval Over ocean Using near-infrared Radiometry. *J. Geophys. Res*. 109: D19106.

Eagan, R.C., Hobbs, P.V. and Radke, L.F. (1974). Measurements of Cloud Condensation Nuclei and Cloud Droplet Size Distributions in the Vicinity of Forest Fires. *J. Appl. Meteorol.* 13: 553–557.

Eck, T.F., Holben, B. N., Reid, J.S., O'Neill, N.T., Schafer, J.S., Dubovik, O., Smirnov, A., Yamasoe, M.A. and Artaxo, P. (2003). High Aerosol Optical Depth Biomass Burning Events: A Comparison of Optical Properties for Different Source Regions. *Geophys. Res. Lett*. 30: 2035, doi: 10.1029/2003GL017861.

Engelhart, G.J., Hennigan, C.J., Miracolo, M.A., Robinson, A.L. and Pandis, S.N. (2012). Cloud Condensation Nuclei Activity of Fresh Primary and Aged Biomass Burning Aerosol. *Atmos. Chem. Phys.* 12: 7285–7293.

EPA (2002). *Third External Review Draft of Air Quality Criteria for Particulate Matter,* USEPA.

Essenwanger, O.M. (1986). *Elements of Stadistical Analysis*, General Climatology, 1B, Elsevier, Amsterdam, 424 pp.

Feingold, G., Jiang, H. and Harrington, J.Y. (2005). On Smoke Suppression of Clouds in Amazonia. *Geophys.*

Res. Lett. 32: L02804, doi: 10.1029/2004GL021369.

Fernandez-Gonzalez, S., del Rio, S., Castro, A., Penas, A., Fernandez-Raga, M., Calvo, A.I. and Fraile, R. (2012). Connection between NAO, Weather Types and Precipitation in León, Spain (1948-2008). *Int. J. Climatol*. 32: 2181–2196.

Fernandez-Raga, M., Fraile, R., Keizer, J.J., Varela-Teijeiro, M.E., Castro, A., Palencia, C., Calvo, A.I., Koenders, J. and Marques, R.L. (2010). The Kinetic Energy of Rain Measured with an Optical Disdrometer: An Application on Splash Erosion. *Atmos. Res*. 96: 225–240.

Formenti, P., Boucher, O., Reiner, T., Sprung, D., Andreae, M.O., Wendisch, M., Wex, Kindred, H.D., Tzortziou, M., Vasaras, A. and Zerefos, C. (2002). STAAARTE-MED 1998 Summer Airborne Measurements over the Aegean Sea: 2. Aerosol Scattering and Absorption, and Radiative Calculations. *J. Geophys. Res.* 107: 4451, doi: 10.1029/2001JD001536.

Fraile, R., Calvo, A.I., Castro, A., Fernandez-Gonzalez, D. and Garcia-Ortega, E. (2006). The Behavior of the Atmosphere in Long-range Transport. *Aerobiologia* 22: 35–45.

Guyon, P., Boucher, O., Graham, B., Beck, J., Mayol-Bracero, O.L., Roberts, G.C., Maenhaut, W., Artaxo, P. and Andreae, M.O. (2003). Refractive Index of Aerosol Particles over the Amazon Tropical Forest during LBA-EUSTACH 1999. *J. Aerosol Sci*. 34: 883–907.

Hodzic, A., Madronich, S., Bohn, B., Massie, S., Menut, L. and Wiedinmyer C. (2007). Wildfire Particulate Matter in Europe during Summer 2003: Meso-scale Modeling of Smoke Emissions, Transport and Radiative Effects. *ACP* 7: 4043–4064.

Hoppel, W.A., Frick, G.M., Fitzgerald, J. and Larson, R.E. (1994). Marine Boundary-layer Measurements of New Particle Formation and the Effects Non-precipitating Clouds Have on Aerosol Size Distribution. *J. Geophys. Res*. 99: 14,443–14,459.

IPCC (2001). Climate Change 2001: The Scientific Basis, Cambridge University Press.

IPCC (2007). Climate Change 2007: Synthesis Report, In *Contribution of Working Groups I, II and III to the Fourth Assessment Report of the Intergovernmental Panel on Climate Change*, Pachauri, R.K. and Reisinger, A. (Eds.), IPCC, Geneva, Switzerland.

Janhall, S., Andreae, M.O. and Poschl, U. (2010). Biomass Burning Aerosol Emissions from Vegetation Fires: Particle Number and Mass Emission Factors and Size Distributions. *Atmos. Chem. Phys*. 10: 1427–1439.

Jenkinson, A.F. and Collison, F.P. (1977). *An Initial Climatology of Gales over the North Sea*, Synoptic Climatology Branch Memorándum, 62, Meteorological Office, London.

Jiang, H. and Feingold, G. (2006). Effect of Aerosol on Warm Convective Clouds: Aerosol-cloud-surface Flux Feedbacks in a New Coupled Large Eddy Model. *J. Geophys. Res.* 111: D01202, doi: 10.1029/2005JD006138.

Jones, P.D., Hulme, M. and Briffa, K.R. (1993). A Comparison of Lamb Circulation Types with an Objective Classification Scheme. *Int. J. Climatol*.13: 655–663.

Kim, Y.J. and Boatman, J.F. (1990). Size Calibration Corrections for the Active Scattering Aerosol Spectrometer Probe (ASASP-100X). *Aerosol Sci. Technol*. 12: 665–672.

Kleeman, M.J., Schauer, J.J. and Cass, G.R. (1999). Size and Composition Distribution of Fine Particulate Matter Emitted from Wood Burning, Meat Charbroiling, and Cigarettes. *Environ. Sci. Technol*. 33: 3516–3523.

Lamb, H.H. (1972). *British Isles Weather Types and a Register of Daily Sequence of Circulation Patterns, 1861-1971*. Geophysical Memoir 116, HMSO, London.

Le Canut, P., Andreae, M.O., Harris, G.W., Wienhold, F.G. and Zenker, T. (1996). Airborne Studies of Emissions from Savanna Fires in Southern Africa 1. Aerosol Emissions Measured with a Laser Optical Particle Counter. *J. Geophys. Res*. 101: 23615–23630.

Londahl, J., Pagels, J., Boman, C., Swietlicki, E., Massling, A., Rissler, J., Blomberg, A., Bohgard, M. and Sandström, T. (2008). Deposition of Biomass Combustion Aerosol Particles in the Human Respiratory Tract. *Inhalation Toxicol.* 20: 923–933.

Lyamani, H., Olmo, F.J., Alcántara, A., Alados-Arboledas, L. (2006). Atmospheric Aerosols during the 2003 Heat Wave in Southeastern Spain II: Microphysical Columnar Properties and Radiative Forcing. *Atmos. Res*. 40: 6465–6476.

Makela, J.M., Koponen, I., Aalto, P. and Kulmala, M. (2000). One-year Data of Submicron Size Modes of Tropospheric Background Aerosol in Southern Finland. *J. Aerosol Sci*. 31: 595–611.

Malavelle, F., Pont, V., Mallet, M., Solmon, F. and Johnson, B. (2011). The West African Aerosols through DABEX and AMMA SOP-0 Campaigns: Simulation of the Atmospheric Loading, Direct Radiative Forcing and Resolute Heating Rates during the Dry Season. *J. Geophys. Res*. 116: D08205, doi: 10.1029/2010JD014829.

Mallet, M., Pont, V., Liousse, C., Gomes, L., Pelon, J., Osborne, S., Haywood, J., Roger, J.C., Dubuisson, P., Mariscal, A., Thouret, V. and Goloub, P. (2008). Aerosol Direct Radiative Forcing over Djougou (Northern Benin) during the African Monsoon Multidisciplinary Analysis Dry Season Experiment (Special Observation Period-0). *J. Geophys. Res.* 113: D00C01, doi: 10.1029/2007JD009419.

Mallet, M., Tulet, P., Serça, D., Solmon, F., Dubovik, O., Pelon, J., Pont, V., Lohou, F. and Thouron, O. (2009). An Impact of Dust Aerosols on Direct Radiative Forcing, Surface Energy Budget, Heating Rate Profiles and Convective Activity over West Africa during March 2006. *Atmos. Chem. Phys.* 9: 7143–7160.

Martins, J., Gonçalves, F., Morales, C., Fisch, G., Pinheiro, F., Leal Junior, J., Oliveira, C., Silva, E., Oliveira, J.C., Costa, A. and Silva Dias, M. (2009). Cloud Condensation Nuclei from Biomass Burning during the Amazonian Dry-to-wet Transition Season. *Meteorol. Atmos. Phys.* 104: 83–93.

Oberdarster, G., Oberdarster, E. and Oberdarster, J. (2005). Nanotoxicology: An Emerging Discipline Evolving from Studies of Ultrafine Particles. *Environ. Health Perspect*. 113: 823–839.

Pere, J.C., Mallet, M., Pont, V. and Bessagnet, B. (2011).

Impact of Aerosol Direct Radiative Forcing on the Radiative Budget, Surface Heat Fluxes, and Atmospheric Dynamics during the Heat Wave of Summer 2003 over Western Europe: A Modeling Study. *J. Geophys. Res.* 116: D23119, doi: 10.1029/2011JD016240.

Petters, M.D., Carrico, C.M., Kreidenweis, S.M., Prenni, A.J., DeMott, P.J., Collett Jr., J.L. and Moosmüller, H. (2009). Cloud Condensation Nucleation Activity of Biomass Burning Aerosol. *J. Geophys. Res*. 114: D22205, doi: 10.1029/2009JD012353.

Radke, L.F., Hegg, A.S., Hobbs, P.V. and Pender, J.E. (1995). Effects of Aging on the Smoke from a Large Forest Fire. *Atmos. Res*. 38: 315–332.

Reid, J.S. and Hobbs, P.V. (1998). Physical and Optical Properties of Smoke from Individual Biomass Fires in Brazil. *J. Geophys. Res*. 103: 32013–32031.

Reid, J.S., Eck, T.F., Christopher, S.A., Koppmann, R., Dubovik, O., Eleuterio, D.P., Holben, B.N., Reid, E.A. and Zhang, J. (2005). A Review of Biomass Burning Emissions Part III: Intensive Optical Properties of Biomass Burning Particles. *Atmos. Chem. Phys*. 5: 827–849.

Remer, L.A., Kaufman, Y.J., Holben, B.N., Thompson, A.M. and McNamara, D. (1998). Biomass Burning Aerosol Size Distribution and Modeled Optical Properties. *J. Geophys*. Res. 103: 31879–31891.

Riley, W.J., McKone, T.E., Lai, A.C.K. and Nazaroff, W.W. (2001). Indoor Particulate Matter of Outdoor Origin: Importance of Size-Dependent Removal Mechanisms. *Environ. Sci. Technol*. 36: 200–207.

Rissler, J., Vestin, A., Swietlicki, E., Fisch, G., Zhou, J., Artaxo, P. and Andreae, M.O. (2006). Size Distribution and Hygroscopic Properties of Aerosol Particles from Dry-season Biomass Burning in Amazonia. *Atmos. Chem. Phys*. 6: 471–491.

Roberts, G.C., Artaxo, P., Zhou, J., Sweitlicki, E. and Andreae, M.O. (2002). Sensitivity of CCN Spectra on Chemical and Physical Properties of Aerosol: A Case Study from the Amazon Basin. *J. Geophys. Res*. 107: 8070, doi: 10.1029/2001JD000583.

Seinfeld, J.H. and Pandis, S.N. (1998). *Atmospheric Chemistry and Physics: From Air Pollution to Climate Change*, John Wiley & Sons, Inc.

Sicard, M., Mallet, M., Garcia-Vizcaino, D., Comeron, A., Rocadenbosch, F., Dubuisson, P. and Munoz-Porcar, C. (2012). Intense Dust and Extremely Fresh Biomass Burning Outbreak in Barcelona, Spain: Characterization of Their Optical Properties and Estimation of Their Direct Radiative Forcing. *Environ. Res. Lett.* 7: 034016, doi: 10.1088/1748-9326/7/3/034016.

Stamnes, K., Tsay, S.C., Wiscombe, W. and Jayaweera, K. (1988). Numerically Stable Algorithm for Discrete-Ordinate-method Radiative Transfer in Multiple Scattering and Emitting Layered Media. *Appl. Opt.* 27: 2502–2509.

Thatcher, T.L. and Layton, D.W. (1995). Deposition, Resuspension, and Penetration of Particles within a Residence. *Atmos. Environ*. 29: 1487–1497.

Tomás, C., De Pablo, F. and Rivas Soriano, L. (2004). Circulation Weather Types and Cloud-to-ground Flash Density over the Iberian Peninsula. *Int. J. Climatol*. 24: 109–123.

Trigo, R.M. and DaCamara, C.C. (2000). Circulation Weather Types and Their Influence on the Precipitación Regime IN Portugal. *Int. J. Climatol*. 20: 1559–1581.

Vakeva, M., Hameri, K., Puhakka, T., Nilsson, E.D., Holiti, H. and Makela, J.M. (2001). Effects of Meteorological Processes on Aerosol Particle Size Distribution in an Urban Background Area. *J. Geophys. Res*. 105: 9807–9821.

Warner, J. and Twomey, S. (1967). The Production of Cloud Nuclei by Cane Fires and The effect on Cloud Drop Concentrations. *J. Atmos. Sci*. 24: 704–713.

Whitby, K.H. (1978). The Physical Characteristics of Sulphur Aerosols. *Atmos. Environ*. 12: 135–159.

Received for review, May 17, 2013
Accepted, October 7, 2013